HIGH-FIDELITY DAMAGE ANALYSIS OF COMPOSITES USING A PLY-BASED CONTINUUM MODEL

Italian Association of Aeronautics and Astronautics
XXV International Congress
9-12 September 2019 | Rome, Italy

HIGH-FIDELITY DAMAGE ANALYSIS OF COMPOSITES USING A PLY-BASED CONTINUUM MODEL

M. H. Nagaraj[1], J. Reiner[2], R. Vaziri[2], E. Carrera[1*] and M. Petrolo[1]

[1]MUL[2] Group, Department of Mechanical and Aerospace Engineering, Politecnico di Torino, Corso Duca degli Abruzzi 24, Torino, Italy

[2] Composites Research Network, The University of British Columbia, Vancouver, Canada

E-mail: manish.nagaraj@polito.it, hannes.reiner@composites.ubc.ca, reza.vaziri@ubc.ca, erasmo.carrera@polito.it, marco.petrolo@polito.it

ABSTRACT

The current work is based on the implementation of the CODAM2 intralaminar damage model in CUF-Explicit, an explicit nonlinear dynamics solver based on the Carrera Unified Formulation (CUF). The CODAM2 model is based on the concept of continuum damage mechanics, and stress-based failure criteria are used to determine the onset of damage. The damage progression makes use of the crack-band theory to scale the fracture energies, thus ensuring mesh objectivity. The structural modelling is performed using high-order 2D theories based on CUF. 2D elements are used to model the structural geometry, and 1D expansions based on Lagrange polynomials are used to define the thickness, resulting in a layer-wise modelling approach. Numerical assessments are performed considering single elements and tensile coupons. The results are in good agreement with reference numerical solutions and experimental data, thus verifying the current implementation.

Keywords: High-order modelling, CUF, CODAM2, explicit damage modelling

1 INTRODUCTION

Carbon fibre reinforced polymers (CFRP) are a class of advanced materials that are increasingly becoming very popular in the aerospace industry. However, the analysis of such composite structures is difficult since they exhibit multiple complex damage mechanisms and failure modes. This is more evident in numerical analysis, where a high-fidelity model is often required to capture the failure modes necessary to accurately describe both the local and global behaviour of the structure. These issues make the numerical analysis of composite structures, especially on the scale used in industry, a computationally intensive task.

Modelling the material behaviour constitutes a very important aspect of the numerical analysis of composites structures. Various approaches to capture the nonlinear material response have been investigated in recent years. The discrete modelling approach involves techniques such as the Cohesive Zone Method (CZM), where cohesive/interface formulations are used to model intralaminar damage such as matrix cracks, and interlaminar damage such as delamination [1-3]. However, such an approach typically involves significantly high computational costs. An alternative approach, with reduced computational demands, is Continuum Damage Mechanics (CDM). In this technique, the cracks are smeared into the continuum and represented using damage parameters, which account for the softening response in the damaged state. The relatively straightforward implementation and reduced computational costs makes it a widely-

used approach [4-6]. A popular method for numerical damage analysis is the use of CDM-based models for intralaminar damage, and a CZM-based approach to model interlaminar damage i.e. delamination. This combines the efficiency of CDM models in representing the effective response of the damaged material while including the effects of delamination, which are critical in scenarios involving transverse loading such as impact of composite structures [7-10].

The current work involves the implementation of the CODAM2 damage model [11] within the framework of the Carrera Unified Formulation (CUF) [12]. CODAM2 is a CDM-based intralaminar damage model, where stress-based failure criteria are used to determine damage initiation, and the damage progression is determined based on the crack-band approach. The mesoscopic form of the CODAM2 damage model [13] has been used in the present work, such that the damage initiation and progression are determined at the ply level. CUF is a generalised framework used to develop advanced structural theories for 1D and 2D models. Expansion functions are used to enrich the kinematics of the cross-section in the case of 1D models, and the thickness in the case of 2D models, which results in 3D-like accuracy of the solution without the corresponding computational costs [14]. The objective of the current work is the explicit damage analysis of composite structures, where the CODAM2 damage model is used to describe the material behaviour and the structural modelling is performed using CUF.

The paper is structured in the following manner. Section 2 describes the CUF framework and the CODAM2 damage model in detail. The numerical assessments and results are discussed in Section 3, and finally the conclusions are given in Section 4.

2 METHODOLOGY

2.1 Carrera Unified Formulation

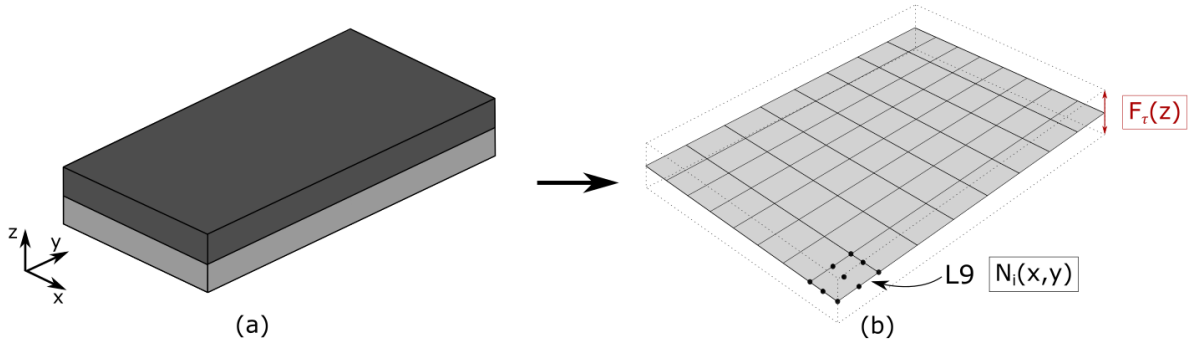

Figure 1: Schematic representation of 2D modelling in CUF

Consider a 2D element aligned in the CUF coordinate system, as shown in Figure 1. The generalized displacement field can be expressed as

$$u(x, y, z) = F_\tau(z) u_\tau(x, y), \tau = 1,2, \dots, M \quad (1)$$

where $F_\tau(z)$ is an expansion function described through the thickness, u_τ is the generalized displacement vector, and M is the number of terms in $F_\tau(z)$. The expansion function and the number of terms M can be arbitrarily chosen and is a user input. The current work uses the Component-Wise (CW) approach, where 1D Lagrange polynomials are used to enhance the through-thickness kinematic field of the 2D finite elements. Such a formulation results in purely displacement degrees of freedom at each node. The displacement field is obtained in the following manner

$$u_x = \sum_{i=1}^{n} F_i(z) u_{xi}(x, y) \tag{2}$$

where *x* denotes the displacement component of a node, and *i* is the node number. Further details on the use of Lagrange-based polynomials as a class of expansion functions may be found in [15].

Finite Element Formulation

The stress and strain fields are given by

$$\boldsymbol{\sigma} = \{\sigma_{xx}\ \sigma_{yy}\ \sigma_{zz}\ \sigma_{xy}\ \sigma_{xz}\ \sigma_{yz}\} \tag{3}$$

$$\boldsymbol{\varepsilon} = \{\varepsilon_{xx}\ \varepsilon_{yy}\ \varepsilon_{zz}\ \varepsilon_{xy}\ \varepsilon_{xz}\ \varepsilon_{yz}\} \tag{4}$$

The linear strain-displacement relation is given by

$$\boldsymbol{\varepsilon} = \mathbf{D}\mathbf{u} \tag{5}$$

where **D** is the linear differentiation operator. The constitutive relation is given by

$$\boldsymbol{\sigma} = \mathbf{C}^{\mathrm{sec}}\boldsymbol{\varepsilon} \tag{6}$$

where $\mathbf{C}^{\mathrm{sec}}$ is the secant stiffness matrix obtained from the CODAM2 material model. Using 2D elements with the shape functions N_i (x, y) to model the in-plane geometry of the structure, the 3D displacement field is written as

$$\mathbf{u}(x, y, z) = F_\tau(z) N_i(x, y) \mathbf{u}_{\tau i} \tag{7}$$

The dynamic equilibrium equation is solved explicitly using the central difference scheme, whose formulation can be found, for instance, in [16].

2.2 CODAM2 intralaminar damage model

The mesoscopic form of the CODAM2 damage model considers damage initiation and propagation at the ply level. Fibre damage initiation is determined using the following stress-based initiation function

$$F_1 = \frac{\sigma_{11}}{X_T} \tag{8}$$

where σ_{11} is the longitudinal stress and X_T is the fibre tensile strength. Similarly, matrix damage initiation is determined using the following relation

$$F_2 = \left(\frac{\sigma_{22}}{Y_T}\right)^2 + \left(\frac{\tau_{12}}{S_L}\right)^2 \tag{9}$$

where σ_{22} and τ_{12} are the transverse tensile and shear stresses, respectively. The transverse tensile and shear strengths are denoted by Y_T and S_L, respectively. The equivalent strain ε_α^{eq} in the principal directions are calculated as

$$\varepsilon_1^{eq} = |\varepsilon_{11}|,\ \varepsilon_2^{eq} = \sqrt{(\gamma_{12}^e)^2 + (\varepsilon_{22})^2} \tag{10}$$

where γ_{12}^e is the elastic shear strain. The damage saturation strain is given by

$$\varepsilon_1^s = \frac{2g_1^f}{X_T},\ \varepsilon_2^s = \frac{2g_2^f}{T} \tag{11}$$

where g_α^f is the fracture energy density of the constituent material α, and T is the equivalent transverse stress σ_2^{eq} evaluated at $F_2 = 1$ as shown below

$$\sigma_2^{eq} = \frac{\tau_{12}\gamma_{12}^e + \sigma_{22}\varepsilon_{22}}{\sqrt{(\gamma_{12}^e)^2 + (\varepsilon_{22})^2}}\Big|_{F_2=1} \tag{12}$$

Finally, the damage variables are calculated as

$$\omega_\alpha = \left(\frac{\varepsilon_\alpha^{eq} - \varepsilon_\alpha^i}{\varepsilon_\alpha^s - \varepsilon_\alpha^i}\right)\left(\frac{\varepsilon_\alpha^s}{\varepsilon_\alpha^{eq}}\right), \alpha = 1,2 \tag{13}$$

where ε_α^i is the failure initiation strain i.e. $\varepsilon_\alpha^{eq}|_{F_\alpha=1}$. The damage variables ω_α are used to calculate the secant stiffness matrix, which is used in Eq. (6) to calculate the stresses in the damaged state.

3 NUMERICAL RESULTS

3.1 Single-element tests

The initial numerical assessment consists of single-element tests, which are a convenient method to verify the implementation of the damage model. The analysis consists of a single square element of edge-length 1.0 mm, with a nominal ply thickness of 0.125 mm. The material system considered is IM7/8552, whose material properties have been listed in Table 1. The various load cases are discussed as follows:

E_{11} [Gpa]	E_{22} [Gpa]	E_{33} [Gpa]	ν_{12}	ν_{13}	ν_{23}	G_{12} [Gpa]	G_{13} [Gpa]	G_{23} [Gpa]
165.0	9.0	9.0	0.34	0.34	0.5	5.6	5.6	2.8

X_T [MPa]	Y_T [MPa]	S_T [MPa]	G_1^f [kJ/m^2]	G_2^f [kJ/m^2]
2560.0	73.0	90.0	120.0	2.6

Table 1: Material properties of the IM7/8552 system

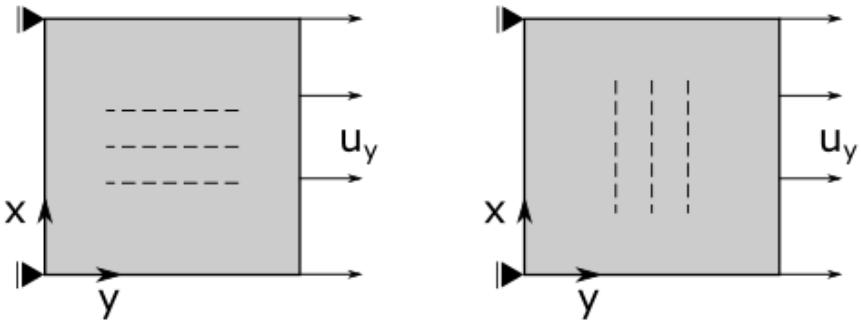

(a) Longitudinal tension (b) Transverse tension

Figure 2: A schematic representation of the single-element tests. (a) tensile load along the fibre, and (b) tensile load transverse to the fibre.

3.1.1 Longitudinal tension

The current assessment consists of a single-element test loaded along the fibre direction, as shown in Figure 2a. In such a case, failure is expected to initiate when the stress reaches a value equal to the fibre strength, which is an input parameter, with a subsequent reduction in the load-bearing capacity. The stress-strain curve of the structure is shown in Figure 3a, which shows that the peak stress in the single-element corresponds to the fibre strength.

3.1.2 Transverse tension

In this case, the tensile load is applied transverse to the fibre direction, as shown in Figure 2b. Under this configuration, the load is carried by the matrix, and failure initiation occurs when the stress reaches the matrix strength. This can be observed in the stress-strain curve plotted in Figure 3b, where the peak stress corresponds to the matrix strength i.e. an input material property.

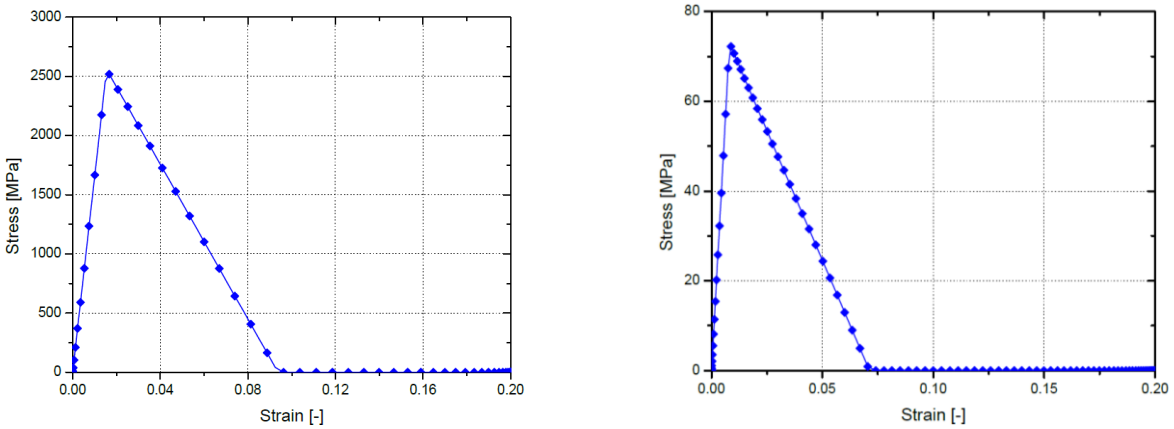

Figure 3: Stress-strain response of the single-element test. (a) longitudinal tension, and (b) transverse tension.

3.1.3 Single-element laminate in tension

The last single-element assessment considers a quasi-isotropic laminate with a stacking sequence of $[90/45/0/-45]_{2s}$, loaded in tension as shown in Figure 4a. In the CUF analysis, each ply has been modelled using a first-order expansion through the thickness, while the in-plane geometry is modelled using a single L4 element. The stress-strain response obtained as a result of the CUF analysis has been plotted in Figure 4b, along with reference numerical solutions obtained from [13].

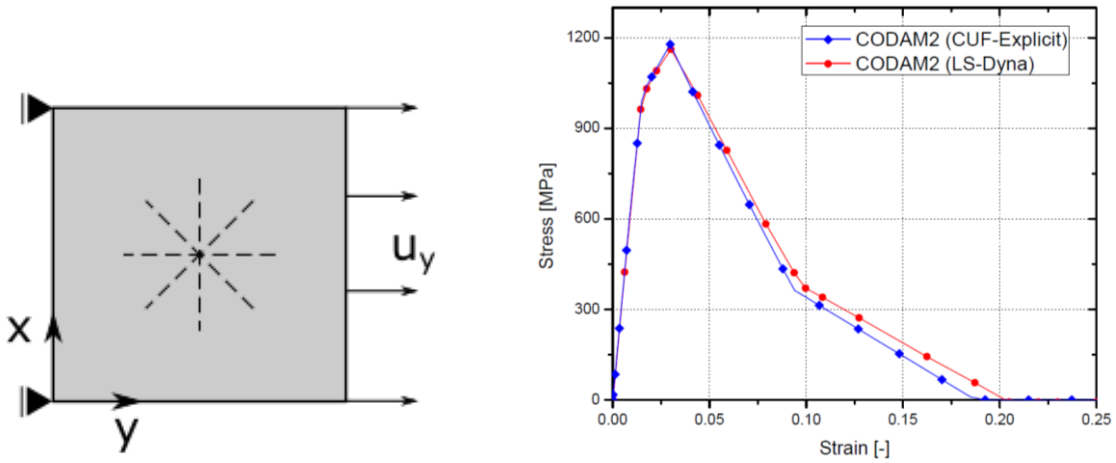

Figure 4: (a) Schematic representation of the quasi-isotropic single-element laminate subjected to a tensile load, and (b) Stress-strain response of the laminate

Some observations can be made

1. The single-element test results verify the current implementation in the CUF framework, as seen in Figure 3.
2. The results obtained from the CUF analysis are in good agreement with those of reference numerical solutions [13], as seen in Figure 4.

3.2 Centre-notched specimen in tension

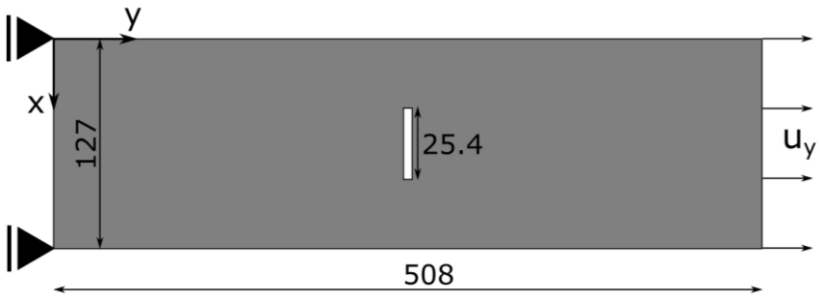

Figure 5: A schematic representation of the centre-notched tensile specimen (dimensions in mm)

The next numerical assessment is that of a coupon-level specimen under tensile loading. A centre-notched specimen has been considered, as shown schematically in Figure 5. The laminate stacking sequence is $[45/90/-45/0]_{4s}$, and the material system is IM7/8552, whose properties have been listed in Table 1. One end of the coupon is clamped, while a displacement $u_y = 3.0$ mm has been prescribed on the opposite end. The structure is based on the scale-8 centre-notched specimen investigated in [13].

The structure is modelled in CUF using 132 L9 elements within the plane of the coupon, with a first-order expansion modelling the thickness of each ply, resulting in a layer-wise model. The results of the CUF analysis has been plotted in the form of the axial stress-strain curve, shown in Figure 6. The figure also shows the curve obtained from reference numerical simulations [13], as well as experimental test results from [17]. The following observations are made

1. The global response predicted by the CUF analysis is in good qualitative agreement with that of the reference numerical results.

2. The peak strength predicted by the CUF analysis matches that given by the reference numerical solution, as well those obtained from experiments.
3. The current approach offers flexibility in terms of structural modelling. The tensile loading of the notched specimen does not require a detailed evaluation of the out-of-plane terms, and therefore a first-order expansion can be used to model each ply. Higher-order expansions can be used when a detailed evaluation of interlaminar stresses are required, such as in the case of delamination.

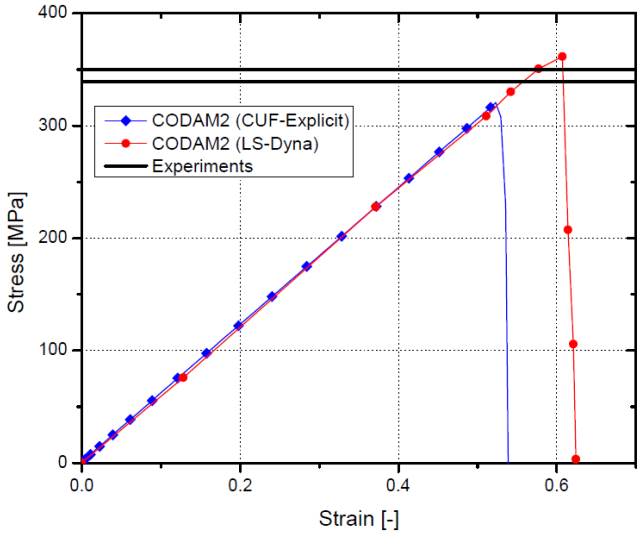

Figure 6: Stress-strain plot of the scale-8 centre-notched specimen in tension

4 CONCLUSION

The current work involved the implementation of the CODAM2 damage model within an explicit dynamics framework based on CUF. High-order theories based on CUF were used to model the geometry of the composite structure, and 1D expansions based on Lagrange polynomials were used to describe the thickness, leading to a layer-wise modelling approach. Numerical assessments such as single-element tests and coupon-level tests on centre-notched tensile specimens were performed. The results indicate that

1. The solutions provided by the CUF analysis are in good agreement with reference solutions, thus verifying the current implementation.
2. The higher-order models available in CUF leads to a high-fidelity and computationally efficient model.
3. In the current approach, differing levels of refinement can be considered for the in- and out-of- plane geometries, which maintains the fidelity of the model as per the requirement of the analysis.

Future works include the development of delamination capabilities, and the use of the current framework in the impact analysis of composite structures.

5 ACKNOWLEDGEMENTS

This research work has been carried out within the project ICONIC (Improving the Crashworthiness of Composite Transportation Structures), funded by the European Union Horizon 2020 Research and Innovation program under the Marie Skłodowska-Curie Grant agreement No. 721256, and the Joint Project for the Internationalization of Research // Polito MUL2 – University of British Columbia.

REFERENCES

[1] L. Lammerant and I. Verpoest. Modelling of the interaction between matrix cracks and delaminations during impact of composite plates. *Composites Science and Technology*, *56*(10), pp.1171-1178 (1996).

[2] F. Aymerich, F. Dore and P. Priolo. Prediction of impact-induced delamination in cross-ply composite laminates using cohesive interface elements. *Composites science and technology*, 68(12), pp.2383-2390 (2008).

[3] X. C. Sun, M. R. Wisnom, and S. R. Hallett. Interaction of inter-and intralaminar damage in scaled quasi-static indentation tests: Part 2–Numerical simulation. *Composite Structures*, 136, pp.727-742 (2016).

[4] A. Matzenmiller, J. Lubliner and R. L. Taylor. A constitutive model for anisotropic damage in fiber-composites. *Mechanics of materials*, *20*(2), pp.125-152 (1995).

[5] L. Iannucci and J. Ankersen. An energy-based damage model for thin laminated composites. *Composites Science and Technology*, *66*(7-8), pp.934-951 (2006).

[6] E. H. Kim, M. S. Rim, I. Lee and T. K. Hwang. Composite damage model based on continuum damage mechanics and low velocity impact analysis of composite plates. *Composite Structures*, *95*, pp.123-134 (2013).

[7] L. Iannucci and M. L. Willows. An energy-based damage mechanics approach to modelling impact onto woven composite materials—Part I: Numerical models. *Composites Part A: Applied Science and Manufacturing*, *37*(11), pp.2041-2056 (2006).

[8] Lopes, C.S., Camanho, P.P., Gürdal, Z., Maimí, P. and González, E.V., 2009. Low-velocity impact damage on dispersed stacking sequence laminates. Part II: Numerical simulations. *Composites Science and Technology*, *69*(7-8), pp.937-947.

[9] L. Maio, E. Monaco, F. Ricci and L. Lecce. Simulation of low velocity impact on composite laminates with progressive failure analysis. *Composite Structures*, *103*, pp.75-85 (2013).

[10] D. Feng and F. Aymerich. Finite element modelling of damage induced by low-velocity impact on composite laminates. *Composite Structures*, *108*, pp.161-171 (2014).

[11] A. Forghani, N. Zobeiry, A. Poursartip and R. Vaziri. A structural modelling framework for prediction of damage development and failure of composite laminates, *J. Comp. Mat.*, Vol. 47, No. 20-21, pp 2553–2573 (2013).

[12] E. Carrera, M. Cinefra, M. Petrolo and E. Zappino. *Finite element analysis of structures through unified formulation*. John Wiley & Sons (2014).

[13] J. Reiner, T. Feser, D. Schueler, M. Waimer and R. Vaziri. Comparison of two progressive damage models for studying the notched behavior of composite laminates under tension. *Composite Structures*, Vol. 207, 385-396 (2019).

[14] A. G. de Miguel, I. Kaleel, M. H. Nagaraj, A. Pagani, M. Petrolo and E. Carrera. Accurate evaluation of failure indices of composite layered structures via various FE models. *Composites Science and Technology, 167*, pp.174-189 (2018).

[15] E. Carrera and M. Petrolo. Refined beam elements with only displacement variables and plate/shell capabilities. *Meccanica, 47*(3), pp.537-556 (2012).

[16] R. De Borst, M. A. Crisfield, J. J. Remmers and C. V. Verhoosel. *Nonlinear finite element analysis of solids and structures*. John Wiley & Sons (2012).

[17] X. Xu, M. R. Wisnom, X. Li and S. R. Hallett. A numerical investigation into size effects in centre-notched quasi-isotropic carbon/epoxy laminates. *Composites Science and Technology, 111*, pp.32-39 (2015).